Photoluminescence of zinc sulfide doped with Mn^{2+} and Eu^{3+} ions in dodecane medium

© L.V. Zatonskaya, V.P. Smagin¶, E.P. Harnutova, E.V. Ignatov

Altai State University,
656049 Barnaul, Russia

¶ E-mail: smaginV@yandex.ru

Received February 21, 2022
Revised February 28, 2022
Accepted February 28, 2022

Photoluminescence (PL) of zinc sulfide powder synthesized and doped with Mn^{2+} and Eu^{3+} ions by the method of emerging reagents in a dodecane medium was investigated. In the absorption and excitation spectra of the PL samples ZnS and $ZnS:Mn^{2+}(Eu^{3+})$, bands corresponding to the transitions of electrons from the valence band to the conduction band and to the levels of structural defects of ZnS, as well as bands of transition of $4f$-electrons of Eu^{3+} ions from the ground $^7F_0$ to excited electronic states were recorded. A wide band associated with recombination processes at the energy levels of defects on the surface of ZnS particles is observed in the PL spectra. Narrow bands of PL are attributed to $^5D_0 \rightarrow {}^7F_j$ and $^4T_1 \rightarrow {}^6A_1$ electronic transitions in Eu^{3+} and Mn^{2+} ions. They are associated with the intra-zone glow centers formed by these ions in the ZnS structure. Energy transfer from ZnS defect levels to excited energy levels of Eu^{3+} ions was registered. Assumptions are made about the mutual influence of ZnS and alloying ions, as well as about the influence of synthesis conditions on the spectral properties of substances.

Keywords: non-aqueous synthesis, dodecane, zinc sulfide, alloying, manganese (II) ions, europium (III) ions, photoluminescence.

DOI: 10.21883/SC.2022.06.53541.9820

1. Introduction

In recent decades, researchers are involved in the development of complex nanometer chemical structures [1–4]. One of the promising semiconductor components and matrices of optical compounds is zinc sulfide [5–7]. Bulky ZnS is well-studied and is used in optical instrument-making as electro- and photoluminescent phosphors [8–10]. Its luminescence is determined by crystal defectiveness. Luminous intensity reaches the maximum in case of a double excess of sulfur ions over zinc ions [11]. The luminescence spectrum is affected by doping with metal ions, state of particle surface, external factors [8,12–16]. As a whole, they define the structure and morphology, as well as the energy diagram which is plotted using the Schen-Klasens and Lambe–Klick schemes.

Thanks to the unique optical properties, lanthanide ions are indispensable components of luminescent materials [17]. In semiconductor matrices they form structural defects that participate in recombination processes. Ln^{3+} also form intraband centers of narrow-band luminescence caused by intra-configuration $^5D_0 \rightarrow {}^7F_j$ transitions of $4f$-electrons [18–22]. Luminescence intensity increases when energy, absorbed by a semiconductor, is transferred to excited levels of Ln^{3+} [21,22]. Moreover, there is a back transfer of energy, which enhances recombination luminescence. Simultaneous occurrence of these processes, if they are not separated by excitation conditions, adversely affects the structures' optical properties.

Mn^{2+} ions, like Ln^{3+} ions, are embedded into semiconductor matrices as optical and magnetic modifiers [10,21,22]. The PL spectra have a band of $^4T_1 \rightarrow {}^6A_1$ electronic transition [9,10,23]. It overlaps the bands of ZnS recombination PL. When concentrations of Mn^{2+} ions are low, a mechanism based on resonance transfer of semiconductor matrix energy to the excited levels of Mn^{2+} ions is implemented. When concentration of Mn^{2+} increases, the „electronic" mechanism becomes predominant. It is related to electron transitions between the „intrinsic" energy levels of Mn^{2+} ions [10]. Only the band of „manganese" luminescence is observed in the spectra of $ZnS:Mn^{2+}$ under selective excitation to the absorption bands of Mn^{2+} ions (390, 435, 470, 496 and 535 nm) [24]. Moreover, Mn^{2+} ions embed into the semiconductor matrix structure and create defects there, whose levels are involved in recombination processes.

Optical properties of semiconductor structures are formed during synthesis and depend on its conditions [1,2,9]. Structures are synthesized using sol-gel technologies, the deposition method, hydrothermal methods [1,5,24–31], films are obtained by different variants of the Langmuir–Blodgett method [1,32]. Synthesis is chiefly carried out in water medium. Sulfidizers are hydrogen sulfide, sodium sulfide and organic sulfur-containing compounds. Supply of gaseous hydrogen sulfide to the reaction medium is not technology-savvy and not environmentally friendly. When sodium sulfide is used, synthesis results to a great extent depend on medium acidity. Hydroxoforms of synthesis products and water molecules quench luminescence and

sometimes suppress it completely (Nd, Eu, Er, Yb). Moreover, the formation of amorphous or partially crystalline phases deteriorates the products' structural homogeneity. When organic sulfur-containing compounds are used as sulfidizers, the product composition to a great extent depends on complexing reactions. The influence of complexes is ambiguous. They deteriorate the state of particle surface, hinder predictability of their size and dimensional dispersion [33]. On the other hand, within compounds they supply additional excitation energy, absorbed by chromophoric groups within ligands.

Several problems could be solved by synthesis in organic media [27,33–38]. The papers [39–42] describe synthesis of transition metal chalcogenides in the medium of high-boiling saturated hydrocarbons in the presence of elemental sulfur. The authors give the results of identification and an estimation of product yield, but their optical properties, possibilities to apply this doping method for making optoelectronic structures were not studied [39–41].

Based on this, our goal was to study photoluminescence of the powder of zinc sulfide synthesized and doped with Mn^{2+} and Eu^{3+} ions in dodecane medium, under excitation of recombination and intraband PL on the particle surfaces.

2. Description of research objects and experimental procedure

Zinc sulfide powder was synthesized by interaction of zinc acetate (chemically pure qualification) with hydrogen sulfide in boiling dodecane (chemically pure qualification) by the method of emerging reagents as per the procedure outlined in [40]. H_2S formed as a result of interaction between elemental sulfur (extra pure) and dodecane during boiling. The process scheme and conditions are given in [40,42]. Doping of ZnS with Mn^{2+} and Eu^{3+} ions was combined with its synthesis. Weighed portions of zinc and europium or zinc and manganese acetates, as well as elemental sulfur were simultaneously added to dodecane. The solution was boiled for 4 h with constant agitation. The weighed portions of manganese and europium acetates were calculated so that the synthesis products had a concentration of Mn^{2+} ions equal to 0.15, 1.5 and 3.0 at%, while that of Eu^{3+} ions — 0.5 and 1.0 at% in relation to the concentration of Zn^{2+} ions. The products were separated by filtering, washed with hot hexane and dried at 80°C. Powders were obtained as a result. The doped powders are colored. Their coloring intensified when the concentration of doping ions increased. The coloring typical for manganese and europium sulfides is associated with an increased concentration of doping ions on the surface of ZnS particles.

The products were identified by X-ray phase analysis using the XRD-6000 unit. The obtained results confirmed the formation of zinc sulfide, which agrees with the data in [39,40]. The doped samples featured a distortion of the crystal lattice parameters of hexagonal ZnS (space group $P6_3mc$, structural type of wurtzite), which confirms embedding of Mn^{2+} and Eu^{3+} ions into its crystal lattice. An amorphous phase was not recorded. The inhomogeneous broadening of reflections is associated with the predominant change of the structure on the particle surface, which corresponds to a change in powder coloring after doping. The electronic spectra of absorption, photoluminescence and photoluminescence excitation of the products were recorded using a Shimadzu RF-5301PC spectrofluorimeter at room temperature.

3. Experimental results and discussion

The photoluminescence spectrum of ZnS under excitation by 360 nm-wavelength radiation has a wide complex band with the maximum in the region of 420–470 nm (Fig. 1, spectrum *1*). Based on its position in the spectrum and the data given in [21,22], it is associated with processes of charge recombination at the level of ZnS crystal structure defects. The increased intensity of this band in the spectra of the $ZnS:Mn^{2+}$ samples, concentration of Mn^{2+} ions being up to 1.5 at%, is due to the growing number of „manganese" defects. Participation of „manganese" defects in recombination processes can be confirmed by an increased intensity of the descending band branch at wavelengths of > 480 nm (Fig. 1, spectra *2, 3, 5*). The decreased intensity of the band (Fig. 1, spectrum *4*) upon an increase in Mn^{2+} ion concentration to 3.0 at% is associated with the growing concentration of MnS, which absorbs the excitation source radiation, on the particle surface. Under excitation by radiation in the region of the absorption band of Mn^2 ions (395 nm), a low-intensity band of $^4T_1 \rightarrow {}^6A_1$ electronic transition (570 nm) was registered in the PL spectrum (Fig. 1, spectrum *5*). Its low intensity is due to the predominant location of Mn^{2+} ions in the near-surface layer and on the surface of ZnS particles in the form of manganese sulfide. A change in the position and contour of the ascending PL band branch (Fig. 1, spectrum *5*,

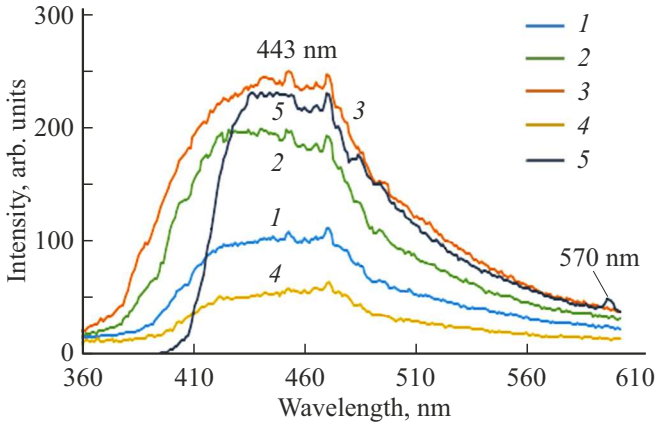

Figure 1. PL spectra ($\lambda_{em} = 360$ nm) of ZnS (*1*) and $ZnS:Mn^{2+}$ for the Mn^{2+} ion concentration equal to, at%: 0.15 (*2*), 1.5 (*3*), 3.0 (*4*), as well as for 1.5 at% at $\lambda_{em} = 395$ nm (*5*).

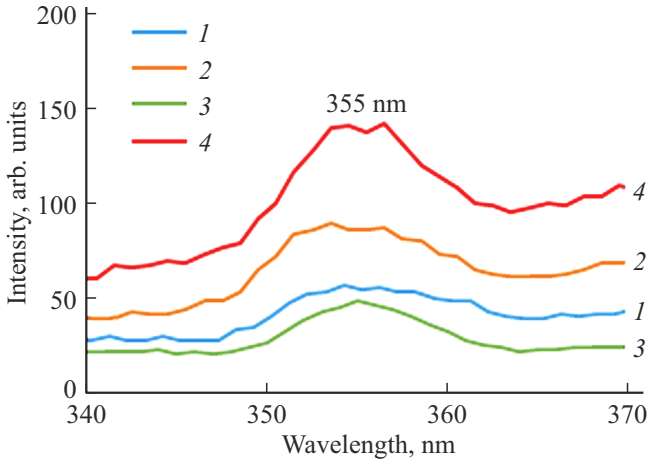

Figure 2. PL excitation spectra ($\lambda_{em} = 469$ nm) of ZnS (*1*) and $ZnS:Mn^{2+}$ for Mn^{2+} ion concentration equal to, at%: 1.5 (*2*), 3.0 (*3*), as well as for 1.5 at% at $\lambda_{em} = 452$ nm (*4*).

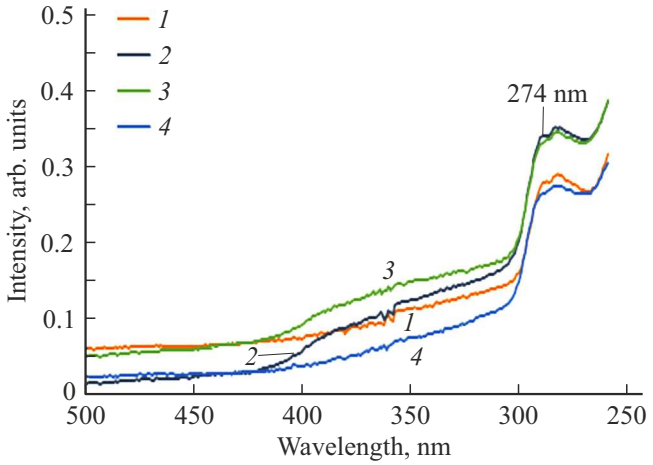

Figure 3. Diffuse reflection spectra of ZnS (*1*), $ZnS:Mn^{2+}$ samples for Mn^{2+} ion concentration, at%: 1.5 (*2*) and 3.0 (*3*), and $ZnS:Eu^{3+}$ sample, $C_{Eu} = 1.0$ at% (*4*).

< 420 nm) is associated with the excitation conditions ($\lambda_{em} = 395$ nm). The observed changes agree with the concepts of influence of Mn^{2+} ions on the PL spectrum of ZnS [9,10,19–22].

The PL excitation spectra for ZnS and $ZnS:Mn^{2+}$ (Fig. 2) have a band with the maximum in the 350–360 nm range. It is associated with electron transition from the valence band to ZnS defect levels. Its position corresponds to the band position in the powders' diffuse reflection spectra in the wavelength range of 300–400 nm (Fig. 3). The band intensity (Fig. 3) is significantly lower than that of the band which corresponds to interband electron transition and is located at wavelengths of < 340 nm ($E_g = 3.68$ eV). The low band intensity is due to the state of the particle surface which forms under the chosen synthesis conditions in dodecane. The change of its intensity in relation to the band of undoped ZnS (Fig. 3, spectra *1–3*) confirms the predominant location of Mn^{2+} ions on the surface of ZnS particles. The decreased intensity of the $ZnS:Eu^{3+}$ band (Fig. 3, spectrum *4*) is explained by the lower concentration of „europium" defects in the surface structure of particles upon a decrease of their concentration in the reaction mixture. The absence of Mn^{2+} and Eu^{3+} ions in the intrinsic band spectra is explained by the low concentration of doping ions in the samples at their typical low absorption coefficients.

The wide band in the PL spectra of the $ZnS:Eu^{3+}$ samples in the wavelength interval of 380–500 nm (Fig. 4) is associated with recombination processes at structural defect levels. They are formed both by matrix ions and by Eu^{3+} ions. The band contour in its short-wave part depends on excitation radiation wavelength (Fig. 4, spectra *1* and *3*, $\lambda_{em} = 360$ nm; spectra 2 and 4, $\lambda_{em} = 395$ nm). The growing band intensity (Fig. 4, spectra *2* and *4*), in relation to spectra *1* and *3* (Fig. 4), corresponds to defect concentration increase in case of a twofold increase of the Eu^{3+} ion concentration. The narrow spectral bands at the wavelengths of > 580 nm are typical for Eu^{3+} ions. They are associated with intra-configuration $^5D_0 \rightarrow {}^7F_j$ transitions of $4f$-electrons. The position of these bands is virtually independent of matrix type. The bands are heterogeneously broadened, particularly in the base, due to the non-equivalence of Eu^{3+} ions' environment. In this respect, the Stark structure of the bands is mild. The low symmetry of Eu^{3+} ions' environment is confirmed by a greater intensity of the band of electrodipole $^5D_0 \rightarrow {}^7F_2$ electronic transition (616 nm), which depends on the symmetry of Eu^{3+} ions' environment, in relation to intensity of the band of magnetic-dipole $^5D_0 \rightarrow {}^7F_1$ electronic transition (593 nm), which is virtually independent of the Eu^{3+} environment symmetry. An increase of the ratio of band intensities in the maxima ($I_{616} : I_{593}$) from 1.9 (Fig. 4, spectra *1* and *3*) to 2.3 (Fig. 4, spectra *2* and *4*) at an increase in the excitation radiation wavelength from 360 nm to 395 nm is explained by a change in the predominant mechanism of Eu^{3+} ion luminescence excitation. Under excitation by 395 nm-wavelength radiation, which matches the most intensive intrinsic absorption band of Eu^{3+} ions ($^7F_0 \rightarrow {}^5L_6$ electronic transition), the excitation process corresponds to the transition of $4f$-electrons via a level systems in the intraband luminescence centers. The presence of a wide recombination luminescence band in the spectrum under such excitation (395 nm) is explained by an overlap of the absorption bands related to electron transition from the valence band to ZnS defect levels (Fig. 1 and 2), and the band of intrinsic absorption transition of Eu^{3+} ions (Fig. 5). The presence of Eu^{3+} ions in the spectra of the intensive luminescence bands under excitation to the matrix absorption band (360 nm) may indicate an energy transfer from levels of ZnS structure defects to excited levels of Eu^{3+} ions, which corresponds to the data in [21,22]. The increased intensity of the luminescence bands of Eu^{3+} ions in spectra *2* and *4* (Fig. 4) in relation to the bands in

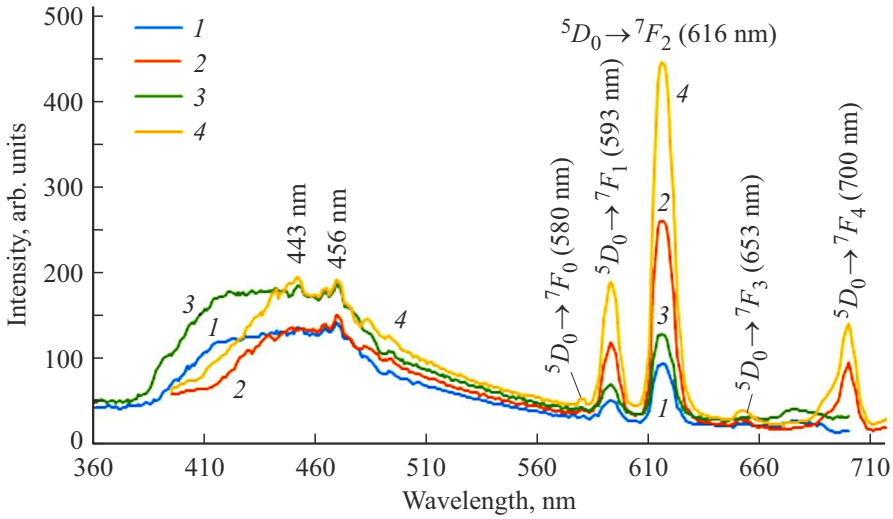

Figure 4. PL spectra of ZnS:Eu^{3+} samples under excitation with 360 nm-wavelength radiation (*1* and *3*) and 395 nm (*2* and *4*), concentration of Eu^{3+} ions 0.5 at% — spectra *1* and *2*, 1.0 at% — spectra *3* and *4*.

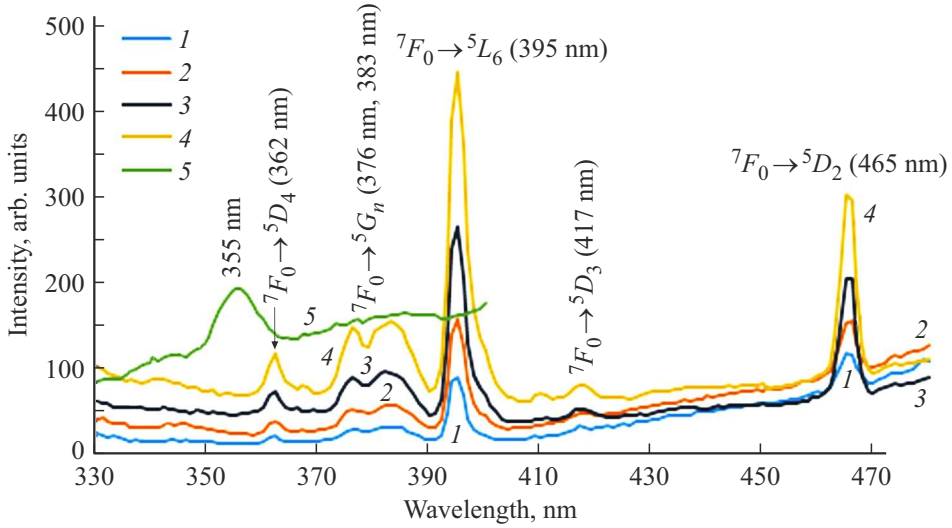

Figure 5. PL excitation spectra of ZnS:Eu^{3+} samples for PL of 594 nm (*1* and *2*), 616 nm (*3* and *4*) and 452 nm (*5*). Concentration of Eu^{3+} ions, at%: 0.5 — spectra *1* and *3*, 1.0 — *2, 4* and *5*.

spectra *1* and *3* (Fig. 4) corresponds to an increase of Eu^{3+} content in the corresponding specimens from 0.5 to 1.0 at%.

A set of bands having different widths and intensities was observed in the PL excitation spectra of the ZnS:Eu^{3+} samples (Fig. 5), recorded for the PL wavelengths associated with Eu^{3+} ions (594 nm, spectra *1* and *2* and 616 nm, spectra *3* and *4*) and with a semiconductor matrix (452 nm, spectrum *5*). The bands associated with electronic transitions of $4f$-electrons of Eu^{3+} ions, prevail in spectra *1–4* (Fig. 5, $\lambda_{em} = 594$ nm and $\lambda_{em} = 616$ nm). Their position coincides with the bands' position in the europium (III) absorption spectrum. Band intensity increases as concentration of Eu^{3+} ions increases. An increase of the background in the 330–360 nm region (spectrum *4*, $\lambda_{em} = 616$ nm) and broadening of the intrinsic excitation bands of Eu^{3+} ions at wavelengths of < 390 nm (Fig. 5) confirms the energy transfer to their excited levels from energy levels of matrix defects.

4. Conclusion

We give the PL study results for zinc sulfide, synthesized and doped with Mn^{2+} and Eu^{3+} ions in dodecane, by interaction of metal acetates with H_2S which forms directly in the reaction medium when elemental sulfur interacts with dodecane at the boiling temperature. A conclusion on predominant doping of the structure on the surface of ZnS particles with Mn^{2+} and Eu^{3+} ions is made based on the analysis of the absorption, excitation and PL spectra. PL

of the $ZnS:Mn^{2+}$ and $ZnS:Eu^{3+}$ samples is associated with recombination processes at the energy levels of intrinsic defects and defects generated by doping ions, as well as with intra-configuration electron transition in the intraband luminescence centers formed by Eu^{3+} and Mn^{2+} ions. It is shown the intraband luminescence is most efficient in case of absorption and emission in the samples doped with Eu^{3+} ions. PL excitation is associated with electron transition from the valence band to ZnS defect levels, as well as under intrinsic absorption of energy by doping ions. We have registered an energy transfer from ZnS defect levels to excited levels of doping ions (Eu^{3+}).

Conflict of interest

The authors declare that they have no conflict of interest.

References

[1] R.F. Khairutdinov. Uspekhi khimii **67** (2), 125 (1998) (in Russian).
[2] A.A. Rempel. Uspekhi khimii **76** (5), 474 (2007) (in Russian).
[3] W. Lu, X. Guo, Y. Luo, Q. Li, R. Zhu, H. Pang. Chem. Eng. J., **355**, 208 (2019).
[4] T.A. Esquivel-Castro, M.C. Ibarra-Alonso, J. Oliva, A. Martínez-Luévanos. Mater. Sci. Eng. C, **96**, 915 (2019).
[5] S.I. Sadovnikov, A.V. Ishchenko, I.A. Vanshtein. Zhurn. neorgan. khimii, **65** (9), 1183 (2020) (in Russian).
[6] E. Ramya, M.V. Rao, D.N. Rao. Physica E: Low-Dim. Systems and Nanostructures, **107**, 24 (2019).
[7] S. Kumar, R. Bhushan, S.R. Kumar, S. Rajpal. Chalcogenide Lett., **19**, 1 (2022).
[8] O.N. Kazankin, L.Ya. Markovsky, I.A. Mironov, F.M. Pekerman, L.N. Petoshina. *Neorganicheskie lyuminofory* (L., Khimiya, 1975) (in Russian).
[9] R.N. Bhargava, D. Gallagher, X. Hong, A. Nurmikko. Phys. Rev. Lett., **72**, 416 (1994).
[10] M.F. Bulanyi, B.A. Polezhaev, T.A. Prokofiev. FTP, **32** (6), 673 (1998) (in Russian).
[11] V.G. Korsakov, M.M. Sychev, V.V. Bakhmetiev. Kondensirovannye sredy i mezhfaznye granitsy, **14** (1), 41 (2012) (in Russian).
[12] T.A. Kuchakova, G.V. Vesna, V.A. Makar. FTP, **38** (11), 1316 (2004) (in Russian).
[13] N.K. Morozova, I.A. Karetnikov, D.A. Mideros, E.M. Gavrishchuk, V.B. Ikonnikov. FTP, **40** (10), 1185 (2006) (in Russian).
[14] K.A. Ogurtsov, M.M. Sychev, V.V. Bakhmetiev, V.N. Korobko, A.I. Ponyayev, F.I. Vysikailo, V.V. Belyayev. Neorg. mater., **52** (11), 1188 (2016) (in Russian).
[15] M. Masab, H. Muhammad, F. Shah, M. Yasir, M. Hanif. Mater. Sci. Semicond. Process., **81**, 113 (2018).
[16] A.A. Othman, M.A. Osman, M.A. Ali, W.S. Mohamed, E.M.M. Ibrahim. J. Mater. Sci.: Mater. Electron., **31**, 1752 (2020).
[17] G.H. Dieke. *Spectra and energy levels of rare earth in crystals* (N.Y. Interscience Publ., 1968).
[18] P. Mukherjee, R.F. Sloan, Ch.M. Shade, D.H. Waldeck, S. Petoud. J. Phys. Chem. C, **117** (27), 14451 (2013).
[19] Z. Liang, J. Mu, L. Han, H. Yu. J. Nanomaterials, Article ID 519303 (2015).
[20] Q. Chen, J. Song, Ch. Zhou, Q. Pang, L. Zhou. Mater. Sci. Semicond. Process., **46**, 53 (2016).
[21] Yu.G. Galyametdinov, D.O. Sagdeev, V.K. Voronkova, A.A. Sukhanov, R.R. Shamilov. Izv. RAN. Ser. khim., **67** (1), 172 (2018) (in Russian).
[22] D.O. Sagdeev. Synopsis of PhD thesis. (Kazan, KNRTU, 2019) (in Russian).
[23] N.H. Patel, M.P. Deshpande, S.H. Chaki, H.R. Keharia. J. Mater. Sci.: Mater. Electron., **28** (15), 10866 (2017).
[24] M.F. Bulanyi, A.V. Kovalenko, B.A. Polezhaev, T.A. Prokofiev. FTP, **43** (6), 745 (2009) (in Russian).
[25] B.N. Litvin, V.I. Popolitov. *Gidrotermalnyi sintez neorganicheskikh soedineniy* (M., Nauka, 1984) (in Russian).
[26] D. Denzler, M. Olschewski, K. Sattler. J. Appl. Phys., **84** (5), 2841 (1998).
[27] K.Yu. Ponomareva, I.D. Kosobudsky, E.V. Tretyachenko, G.Yu. Yurkov. Neorg. mater., **43** (11), 1295 (2007) (in Russian).
[28] M. Kuzmanović, D.K. Bozanić, D. Milivojević, D.M. Ćulafić, S. Stanković, C. Ballesteros, J. Gonzalez-Benito. RSC Advances, **7** (84), 53422 (2017).
[29] C. Rosiles-Perez, J. Lambert, A. Alatorre-Ordaz, J.A. Gutierrez, T. Lopez-Luke, R. Ramirez-Fuentes, T. Kobayash. J. Luminesc., **184**, 123 (2017).
[30] N.S.M. Mustakim, Ch.A. Ubani, S. Sepeai, N.A. Ludin, M.A.M. Teridi, M.A. Ibrahim. Solar Energy, **163**, 256 (2018).
[31] P. Kunstman, J. Coulon, O. Kolmykov, Hatem Moussa, Lavinia Balan, Ghouti Medjahdi, Janina Lulek, Raphaël Schneider. J. Luminesc., **194**, 760 (2018).
[32] A.A. Zarubanov, K.S. Zhuravlev. FTP, **49** (3), 392 (2015) (in Russian).
[33] V.P. Smagin, D.A. Davydov, N.M. Unzhakova, A.A. Biryukov. Zhurn. neorgan. khimii, **60** (12), 1734 (2015) (in Russian).
[34] I.A. Akimov, I.Yu. Denisyuk, A.M. Meshkov. Opt. i spektr., **72** (4), 1026 (1992) (in Russian).
[35] L. Pedone, E. Caponetti, M. Leone. J. Colloid and Interface Sci., **284**, 495 (2005).
[36] A.A. Biryukov, T.I. Izaak, V.A. Svetlichny, O.V. Babkina. Izv. vuzov. Fizika, **49** (12), 81 (2006) (in Russian).
[37] A.A. Isaeva, V.P. Smagin. FTP, **54** (12), 1321 (2020) (in Russian).
[38] V.P. Smagin, A.A. Isaeva. Pis'ma ZhTF, **47** (16), 46 (2021) (in Russian).
[39] E.I. Perov, E.P. Irkhina, E.G. Ilyina, I.V. Goncharova, I.S. Fedorov, A.N. Golovachev. *Sposob polucheniya sulfida metalla* (in Russian). Patent RU 2112743.
[40] E.P. Irkhina. Synopsis of PhD thesis. (Barnaul, AltSU, 2000) (in Russian).
[41] E.I. Perov, E.P. Kharnutova. Izv. Alt. gos. un-ta, **3–2** (67), 186 (2010) (in Russian).
[42] E.P. Kharnutova, L.V. Zatonskaya, V.P. Smagin, E.G. Ilyina. Polzunovsky vestn., **2**, 113 (2020) (in Russian).